Charge Migration in Propiolic Acid: A Full Quantum Dynamical Study

Victor Despré,[1,*] Nikolay V. Golubev,[1] and Alexander I. Kuleff[1,2,†]
[1]Theoretische Chemie, PCI, Universität Heidelberg, Im Neuenheimer Feld 229, D-69120 Heidelberg, Germany
[2]ELI-ALPS, Budapesti út 5, H-6728 Szeged, Hungary

(Received 24 July 2018; published 16 November 2018)

Ionization of molecules very often populates several cationic states launching pure electron dynamics that appear as ultrafast migration of the hole charge throughout the system. A crucial question in the emerging field of attochemistry is whether these pure electronic coherences last long enough to allow for their efficient observation and eventual manipulation with ultrashort laser pulses. We report a full-dimensional quantum calculation of concerted electron-nuclear dynamics initiated by outer-valence ionization of propiolic acid molecule, showing that the charge will oscillate between the carbon triple bond and the carbonyl oxygen for more than 10 fs before getting trapped by the nuclear motion. This time is enough for the charge migration to be observed and controlled. We argue that the molecule is very suitable for experimental studies.

DOI: 10.1103/PhysRevLett.121.203002

The attosecond-laser-technology revolution [1,2] has made it possible to study electronic dynamics on their intrinsic timescale [3,4]. Ultrafast rearrangements of the electronic cloud of molecules triggered by external perturbation can now be followed in time. It has been predicted theoretically [5] that very often ionization of a molecule can lead to a coherent population of cationic states launching in that way pure electronic dynamics in which the created hole charge can migrate throughout the system on an ultrashort timescale [6]. First time-resolved measurements of pure electronic coherences following ionization of complex molecular systems have already been reported [7–9]. One of the most important open questions in the field of ultrafast science, however, is how long the pure electronic dynamics last [10–15]. Recent theoretical studies have shown that in some cases the nuclear motion can make the electronic coherence disappear extremely fast [14,15]. Moreover, it was argued that even a large difference in the timescales of electron and nuclear motion is not sufficient to insure a long-lasting electronic coherence, and even small nuclear displacements can induce loss of coherence in complex molecules within 1–2 fs, due to the interplay of many vibrational modes [15].

The question of electronic-coherence time span is of particular importance, because if the pure electron dynamics lasts long enough it can be manipulated by specifically tailored ultrashort pulses [16–18], potentially influencing the follow-up nuclear rearrangement and thus the chemical reactivity of the molecule. The possibility of such control lies in the heart of what became to be known as "attochemistry." The paradigm of attochemistry is that a particular reaction path of the molecule can be preselected at a very early stage of its quantum evolution by acting only on the electronic degrees of freedom (d.o.f.) before the nuclei have time to move significantly. Because of the coupling between the electronic and nuclear motion, by controlling the electronic coherence one will indirectly steer the succeeding structural changes of the molecular skeleton. In the case of charge migration, such reaction control can be achieved by redistributing the charge in such a way during the pure electron-dynamics step that the desired nuclear rearrangement is then triggered. This can be done, however, only if the electronic coherences last long enough to be efficiently manipulated.

Using a fully quantum approach to treat the coupled electron-nuclear dynamics, here we demonstrate that longer-lived electronic coherences may exist even in complex polyatomic molecules. This is exemplified on propiolic acid (HC_2COOH) showing that the charge created upon ionization out of the highest occupied molecular orbital (HOMO) will oscillate between the carbon triple bond and the carbonyl oxygen for more than 10 fs before being trapped by the nuclear motion. This time is enough for performing an efficient control over the charge migration dynamics [18].

In order to describe the concerted electron-nuclear dynamics in ionized molecules, we have to go beyond the Born-Oppenheimer approximation. A possible way to do this, while still keeping the convenient notion of electronic states, is to use the formally exact Born-Huang expansion [19] of the molecular wave function

$$\Psi(\mathbf{r},\mathbf{R},t)=\sum_i \chi_i(\mathbf{R},t)\Phi_i(\mathbf{r},\mathbf{R}), \tag{1}$$

where $\mathbf{r}$ and $\mathbf{R}$ denote all electronic and nuclear coordinates, respectively, $\Phi_i(\mathbf{r},\mathbf{R})$ are the full set of eigenfunctions of the electronic Hamiltonian (the full molecular

Hamiltonian with the nuclear kinetic energies set to zero), and the expansion coefficients $\chi_i(\mathbf{R},t)$ are the time-dependent nuclear wave packets. Within ansatz (1), the time-dependent Schrödinger equation transforms into a set of coupled equations for the nuclear wave packets propagating on the electronic potential-energy surfaces (PES). The latter are built up by solving the electronic eigenvalue problem at each set of nuclear coordinates $\mathbf{R}$.

Because of the nonadiabatic couplings, however, it is quite cumbersome to solve the resulting equations of motion using the adiabatic electronic states and that is why very often the equations are reformulated in the so-called diabatic electronic basis, whose dependence on the nuclear coordinates is so small that the derivative couplings are either negligible [20] or completely vanishing [21]. For bound electronic states, such reformulation of the problem can be done through the vibronic-coupling Hamiltonian model [22], based on a Taylor expansion of the PESs around the energy minimum. By transforming from adiabatic to diabatic representation, the coupling between the electronic states changes from derivative coupling to coordinate coupling appearing as off-diagonal elements in the potential-energy matrix. With the resulting vibronic-coupling Hamiltonian we can propagate the nuclear wave packets created by the initial ionization. We note that usually these types of computations are performed by propagating a single nuclear wave packet on the PESs, while here, in order to account for the electronic coherences, we need to simultaneously propagate a number of nuclear wave packets on all relevant nonadiabatically coupled electronic states.

Before we turn to the particular case of propiolic acid, we would like to discuss another more general issue, namely, the analysis of the concerted electron-nuclear dynamics following ionization. As we are interested in the process of charge migration, begotten by the initially created electronic coherences, we would like to monitor the evolution of an observable that depends on the electronic d.o.f., like the hole density [5], traditionally used for analysis of charge migration at fixed nuclear geometry [6].

The expectation value of a general electronic operator $\hat{O}(\mathbf{r})$ can be written as

$$\langle \hat{O}(t)\rangle = \sum_{i,j} \langle \chi_i(\mathbf{R},t)\Phi_i(\mathbf{r},\mathbf{R})|\hat{O}(\mathbf{r})|\chi_j(\mathbf{R},t)\Phi_j(\mathbf{r},\mathbf{R})\rangle, \tag{2}$$

where the integration is over both the electronic and nuclear coordinates. As $\chi_i(\mathbf{R},t)$ do not depend on the electronic coordinates, we can perform the integration over $\mathbf{r}$ and write

$$\langle \hat{O}(t)\rangle = \sum_{i,j} \langle \chi_i(\mathbf{R},t)|O_{ij}(\mathbf{R})|\chi_j(\mathbf{R},t)\rangle_{\mathbf{R}}, \tag{3}$$

where the integration now is only on the nuclear coordinates and $O_{ij}(\mathbf{R})$ denotes the matrix element of the electronic operator taken between electronic states i and j. We see again that it is advantageous to work in a diabatic representation and use the weak dependence of the diabatic states on $\mathbf{R}$. In this case, Eq. (2) factorizes

$$\langle \hat{O}(t)\rangle = \sum_{i,j} O_{ij}\chi_{ij}(t), \tag{4}$$

where

$$\chi_{ij}(t) = \langle \chi_i(\mathbf{R},t)|\chi_j(\mathbf{R},t)\rangle_{\mathbf{R}}. \tag{5}$$

The quantities $\chi_{ij}(t)$ represent the time-dependent overlaps between the nuclear wave packets evolving on different electronic states [correspondingly $\chi_{ii}(t)$ is the time-dependent population of state i]. Being the only time-dependent quantities in Eq. (4), they are the only source of dephasing of the initially created electronic coherences [14,15] and thus can be used as a measure for the dephasing time. We note here that the coupling between the outgoing electron and the ionic core is another source of decoherence [23]. This effect, however, decreases with the increase of the kinetic energy of the outgoing electron [23].

Using the above sketched formalism, we studied the charge-migration dynamics triggered by outer-valence ionization of the propiolic acid molecule. We showed recently [18] that the ionization out of HOMO will lead to coherent population of the ground and the second excited cationic states of the molecule. This is a consequence of the electron correlation, manifesting in this case as the so-called hole mixing [24], meaning that the populated cationic states are mainly linear combinations of one-hole ($1h$) configurations, corresponding to an electron missing from a particular orbital (see, Refs. [6,24]). In propiolic acid, the orbitals that mix in the first and the third ionic states are $15a'$ (HOMO) and $14a'$ (HOMO-2), which are depicted in the middle panel of Fig. 1. The ionization of HOMO will thus launch charge-migration oscillations between the carbon triple bond and the carbonyl oxygen with a period of about 6.2 fs, determined by the energy gap between the first and the third cationic states [17].

In order to study the decoherence of this charge-migration dynamics introduced by the nuclear motion, we computed the cationic eigenstates of the system along all 15 nuclear d.o.f., using the *ab initio* third-order Algebraic Diagrammatic Construction [ADC(3)] method [25]. At this level of theory, all $1h$ and two-hole–one-particle excitations are taken into account. DZP basis sets [26] were used. A representative example of these calculations is shown in the upper panel of Fig. 1 as dots, where the first four ionic states of the system along the normal vibrational mode of a' symmetry at 462.2 cm^{-1} are depicted. This mode (also sketched in the figure) corresponds mostly to the bending of the carbonyl structure and thus is expected to strongly influence the electron dynamics, as it deforms the

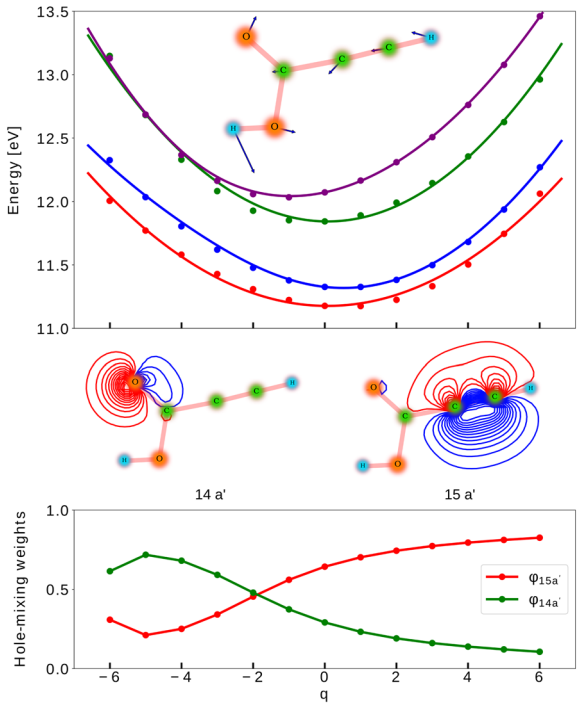

FIG. 1. Top panel: Potential energy surfaces of the first four cationic eigenstates of propiolic acid along the normal mode at 462.2 cm^{-1} belonging to a' symmetry. Adiabatic PESs obtained by Green's function ADC(3)/DZP calculations (dots) and diabatized PESs from the vibronic-coupling model (solid curves) are presented. Middle panel: Molecular orbitals involved in the hole mixing appearing in the ground and the second excited ionic states. Bottom panel: Hole-mixing weights in the ground ionic state along the normal mode shown in the top panel. Horizontal axis of top and bottom panel is the same.

molecular skeleton and the sites between which the charge migration takes place. Importantly, the PESs are relatively parallel to each other, which means that the nuclear wave packets propagating on different cationic states will move mostly synchronously, prolonging the time during which the wave packets significantly overlap in space and thus keep the electronic coherence [see Eq. (4)].

With the help of these adiabatic PESs we constructed a quadratic vibronic-coupling Hamiltonian [27]

$$\hat{H}_{\mathrm{VC}} = \hat{\tau}_N + \nu_0 + W, \tag{6}$$

where $\hat{\tau}_N$ and ν_0 represent the harmonic approximation of the kinetic and potential energy of the neutral unperturbed reference ground state, while the matrix W contains the diabatic energies as diagonal terms and their couplings as off-diagonal elements

$$W_{jj} = E_j + \sum_i \kappa_i^{(j)} q_i + \frac{1}{2}\sum_i \gamma_i^{(j)} q_i^2, \tag{7a}$$

$$W_{jk} = \sum_i \lambda_i^{(jk)} q_i. \tag{7b}$$

In Eqs. (7), E_j is the vertical ionization energy of state j, $\kappa_i^{(j)}$ and $\gamma_i^{(j)}$ are the linear and quadratic couplings of state j for normal mode i, respectively, and $\lambda_i^{(jk)}$ are the linear couplings between states j and k by normal mode i. The quantities q_i are the dimensionless nuclear coordinates, describing the displacement from a reference configuration along the normal mode i. The Hamiltonian $\hat{H}_{\mathrm{VC}}$ takes into consideration the first four states and all the 15 nuclear d.o.f. All parameters of the model are obtained by a least-squares fit with respect to the *adiabatic* PESs computed with the ADC(3) method. An example of the resulting *diabatic* PESs is depicted in the upper panel of Fig. 1 with solid lines. We note that the vibronic couplings between the states $\lambda_i^{(jk)}$ are weak, meaning that there will be very little transfer of population and the different wave packets will mostly propagate on the states where they were initially created. This is a favorable case, as strong couplings and especially conical intersections are a source of decoherence.

We used the vibronic-coupling Hamiltonian to propagate the initial state with the help of the Multi-Configuration Time-Dependent Hartree (MCTDH) method [28,29]. The initial state, corresponding to the removal of a HOMO electron from a vibrationally cold neutral molecule, has been constructed by projecting the ground-state vibrational wave function on the four ionic states of interest using the HOMO hole-mixing weights along all nuclear d.o.f. The hole-mixing weight represents the square of the coefficient with which each orbital participates in the $1h$ part of the corresponding cationic sate. This parameter can change dramatically along a normal mode, as shown in the lower panel of Fig. 1, where the weights, with which orbitals $15a'$ and $14a'$ contribute to the ground ionic state, are depicted along the normal mode at 462.2 cm^{-1}. When both orbitals have a substantial weight in the hole mixing, the electron dynamics will be strong. The strength of hole mixing can be both a source of charge dynamics and a way to suppress it, and can thus operate as a natural filter reducing the dephasing effect of the initial width of the wave packet [11]. Strong electron dynamics will take place only at nuclear configurations where strong hole mixing appears and thus not the full width of the nuclear wave packet will be important for the charge migration.

Before discussing the results of the full molecular dynamics, a comment on the practical realization of such an initial state is in order. In the energy range 11–15 eV only the four states shown in Fig. 1 are present. The first and the third one belong to the a' symmetry, while the second and the forth one to a''. Being a small quasilinear molecule, propiolic acid can be aligned and oriented using, e.g., impulsive orienting techniques [30]. Such a preorientation will permit us to ionize only the symmetry of interest, populating exclusively the ground and the second excited states of the cation. The initial state used in our work also

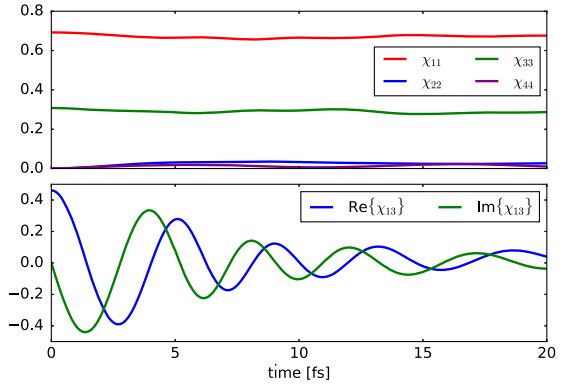

FIG. 2. Time-dependent overlaps of the nuclear wave packets $\chi_{ij}(t)$, Eq. (5), propagating on the first 4 cationic states of propiolic acid after removal of a HOMO electron. Upper panel: The diagonal elements $\chi_{ii}(t)$ giving the population evolution of corresponding states. Lower panel: The real and imaginary part of the most important nondiagonal element $\chi_{13}(t)$ related to the degree of coherence of the system.

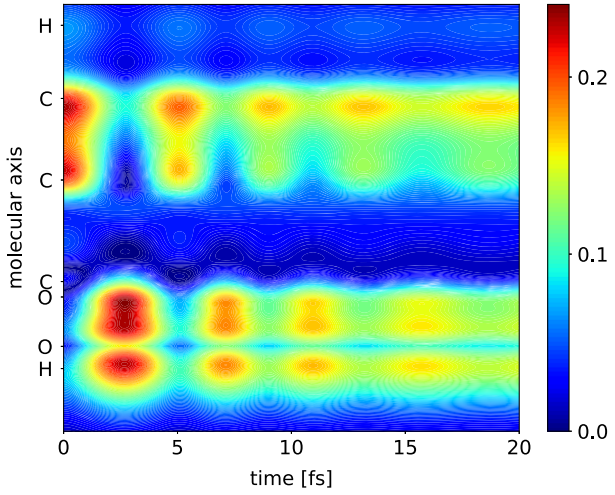

FIG. 3. Time evolution of the hole density, Eq. (8), along the molecular axis of propiolic acid following ionization out of the HOMO. The equilibrium atomic positions are also denoted. The charge-migration oscillations are dephased by the coupling to the nuclear motion. All nuclear d.o.f. are taken into account.

assumes an ultrashort (sudden) ionization. Such a situation can be realized, e.g., by field ionization with a strong IR pulse. Because of the relatively large energy difference between orbitals $15a'$ and $14a'$, the tunnel ionization will be performed nearly exclusively from the HOMO. Ionization with an ultrashort XUV pulse [31] can also be used. The latter scheme has the advantage to create fast photoelectrons, reducing the ionization time to just a few attoseconds [32] realizing in practice the sudden ionization limit (see also Ref. [33]).

Let us now turn to the results of our full-dynamics calculations. Important information about the evolution of the system and the dephasing of the electron coherences can be obtained from the time evolution of the wave packet overlaps $\chi_{ij}(t)$, Eq. (5) [see also Eq. (4)]. Those are presented in Fig. 2. The diagonal elements, or the state populations, are depicted in the upper panel of the figure. As expected, due to the weak vibronic coupling between the states, very small population transfer is observed. The lower panel shows the real and imaginary parts of the nondiagonal element $\chi_{13}(t)$ giving the overlap between the wave packets propagating on the first and third ionic state, and being a measure for the coherence. We see that the system gradually dephases within 20 fs, keeping a high degree of coherence during the first 10 fs. This time is enough for both observing the charge migration and for its control.

Although $\chi_{ij}(t)$ provide information on the lifetime of the electronic coherences, it is important to be able to visualize and analyze the charge dynamics in time and space. A convenient way to do that is to compute the hole density of the system. The latter, defined as the difference between the electronic density of the neutral and that of the cation [5,24], can be constructed from the full molecular wave functions of the system before and after ionization using Eq. (4)

$$Q(\vec{r},t) = \chi_{00}\langle\Phi_0^N|\hat{\rho}|\Phi_0^N\rangle - \sum_{i,j}\chi_{ij}(t)\langle\Phi_i^{N-1}|\hat{\rho}|\Phi_j^{N-1}\rangle, \quad (8)$$

where $\hat{\rho}$ is the electronic density operator, χ_{00} is the overlap integral of the initial vibrational wave function (taken to be 1 as the ground vibrational state is normalized), Φ_0^N is the electronic ground state, and Φ_i^{N-1} are the cationic states. Importantly, to be able to factorize the electronic and nuclear part of the density, we have to use the *diabatic* states.

The hole density computed along the molecular axis of the propiolic acid accounting for all 15 nuclear d.o.f. is shown in Fig. 3. We see that the initial strong charge oscillations between the carbon triple bond and the carboxyl group are gradually damped, distributing the charge. Before being trapped by the nuclear motion, however, the charge performs a few clear oscillations. The time during which the electronic coherence is driving the charge dynamics is, therefore, long enough to allow for an efficient observation and control, making the propiolic acid a suitable candidate for experimental studies.

Before we conclude, we would like to touch upon some of these possibilities. As we mentioned above, due to its linear structure, the pro piolic acid can be aligned and oriented, making it amenable to the time-resolved high-harmonic generation (HHG) technique, employed recently by Wörner and co-workers [8]. The tunnel ionization by a linearly polarized strong IR field will favor removal of a HOMO electron, triggering the charge dynamics discussed above. The increase of intensity will start to admix ionization out of HOMO and HOMO-2, as the probability to tunnel also from the deeper orbital will increase. In such a way, different initial states can be prepared, launching different charge dynamics. Those differences should be encoded in the resulting HHG spectra.

Being able to access only the first few fs after the ionization, the time-resolved HHG spectroscopy would not be very suitable to study the possibility to control the charge-migration dynamics. For this purpose, attosecond XUV-pump–XUV-probe techniques [34] would be more appropriate. Immediately after the pump pulse, the triggered charge migration can be controlled by an IR-pulse sequence, as suggested in Ref. [18]. The delay between the IR pulse and its replica could be optimized to change at will the localization of the hole during the electron dynamics. The degree of control achieved could then be probed by a second ultrashort XUV pulse, e.g., by angle-resolved photoemission spectroscopy, as suggested by Remacle and Levine [35,36], or by time-resolved transient absorption spectroscopy [37]. Although extremely challenging, such experiments would be a proof of concept for the possibilities offered by ultrafast science in terms of control of molecular dynamics and chemical reactivity.

In this Letter we studied the ultrafast charge dynamics initiated by ionization out of the HOMO of propiolic acid. Our fully quantum calculations showed that the electron-correlation driven charge migration survives the decoherence induced by the slower nuclear motion long enough to permit its observation and control. This also shows that pure electronic coherences can last longer even in systems with many nuclear d.o.f. Although certainly very much case dependent, the slower decoherence can be expected in a large number of systems. In this respect, the propiolic acid is not an outlier. Several features of the molecule, however, makes it a suitable candidate for experimental studies, in which the paradigm of attochemistry could be tested. We hope that our work will motivate such investigations.

The authors thank Lorenz Cederbaum for many valuable discussions and Hans Jakob Wörner for drawing our attention to the propiolic acid molecule. Financial support by the DFG through the QUTIF Priority Programme and by the US ARO (Grant No. W911NF-14-1-0383) is gratefully acknowledged. N. V. G. thanks International Max Planck Research School for Quantum Dynamics (IMPRS-QD) (Heidelberg) for financial support.

*victor.despre@pci.uni-heidelberg.de
†alexander.kuleff@pci.uni-heidelberg.de

[1] F. Krausz and M. Ivanov, Rev. Mod. Phys. **81**, 163 (2009).
[2] M. Nisoli, P. Decleva, F. Calegari, A. Palacios, and F. Martín, Chem. Rev. **117**, 10760 (2017).
[3] F. Lépine, M. Y. Ivanov, and M. J. Vrakking, Nat. Photonics **8**, 195 (2014).
[4] S. R. Leone*et al.*, Nat. Photonics **8**, 162 (2014).
[5] L. S. Cederbaum and J. Zobeley, Chem. Phys. Lett. **307**, 205 (1999).
[6] A. I. Kuleff and L. S. Cederbaum, J. Phys. B **47**, 124002 (2014).
[7] F. Calegari *et al.*, Science **346**, 336 (2014).
[8] P. M. Kraus *et al.*, Science **350**, 790 (2015).
[9] H. J. Wörner *et al.*, Struct. Dyn. **4**, 061508 (2017).
[10] V. Despré, A. Marciniak, V. Loriot, M. Galbraith, A. Rouzée, M. Vrakking, F. Lépine, and A. I. Kuleff, J. Phys. Chem. Lett. **6**, 426 (2015).
[11] M. Vacher, L. Steinberg, A. J. Jenkins, M. J. Bearpark, and M. A. Robb, Phys. Rev. A **92**, 040502 (2015).
[12] A. J. Jenkins, M. Vacher, M. J. Bearpark, and M. A. Robb, J. Chem. Phys. **144**, 104110 (2016).
[13] A. J. Jenkins, M. Vacher, R. M. Twidale, M. J. Bearpark, and M. A. Robb, J. Chem. Phys. **145**, 164103 (2016).
[14] M. Vacher, M. J. Bearpark, M. A. Robb, and J. P. Malhado, Phys. Rev. Lett. **118**, 083001 (2017).
[15] C. Arnold, O. Vendrell, and R. Santra, Phys. Rev. A **95**, 033425 (2017).
[16] I. Barth and J. Manz, Angew. Chem. **45**, 2962 (2006).
[17] N. V. Golubev and A. I. Kuleff, Phys. Rev. A **91**, 051401 (2015).
[18] N. V. Golubev, V. Despré, and A. I. Kuleff, J. Mod. Opt. **64**, 1031 (2017).
[19] M. Born and K. Huang, *The International Series of Monographs on Physics* (Oxford University Press, Oxford, 1985).
[20] T. Pacher, L. S. Cederbaum, and H. Köppel, Adv. Chem. Phys. **84**, 293 (1993).
[21] C. A. Mead and D. G. Truhlar, J. Chem. Phys. **77**, 6090 (1982).
[22] H. Köppel, W. Domcke, and L. S. Cederbaum, Adv. Chem. Phys. **57**, 59 (1984).
[23] S. Pabst, L. Greenman, P. J. Ho, D. A. Mazziotti, and R. Santra, Phys. Rev. Lett. **106**, 053003 (2011).
[24] J. Breidbach and L. S. Cederbaum, J. Chem. Phys. **118**, 3983 (2003).
[25] J. Schirmer, A. Trofimov, and G. Stelter, J. Chem. Phys. **109**, 4734 (1998).
[26] A. C. Neto, E. P. Muniz, R. Centoducatte, and F. E. Jorge, J. Mol. Struct. **718**, 219 (2005).
[27] W. Domcke, D. R. Yarkony, and H. Köppel, *Conical Intersections: Theory, Computation and Experiment* (World Scientific, Singapore, 2011), Vol. 17.
[28] H.-D. Meyer, U. Manthe, and L. S. Cederbaum, Chem. Phys. Lett. **165**, 73 (1990).
[29] M. H. Beck, A. Jäckle, G. Worth, and H.-D. Meyer, Phys. Rep. **324**, 1 (2000).
[30] H. Stapelfeldt and T. Seideman, Rev. Mod. Phys. **75**, 543 (2003).
[31] M. Chini, K. Zhao, and Z. Chang, Nat. Photonics **8**, 178 (2014).
[32] A. Maquet, J. Caillat, and R. Taïeb, J. Phys. B **47**, 204004 (2014).
[33] A. I. Kuleff and L. S. Cederbaum, Phys. Rev. Lett. **106**, 053001 (2011).
[34] T. Barillot, P. Matia-Hernando, D. Greening, D. Walke, T. Witting, L. Frasinski, J. Marangos, and J. Tisch, Chem. Phys. Lett. **683**, 38 (2017).
[35] B. Mignolet, R. D. Levine, and F. Remacle, Phys. Rev. A **86**, 053429 (2012).
[36] T. Kuś, B. Mignolet, R. D. Levine, and F. Remacle, J. Phys. Chem. A **117**, 10513 (2013).
[37] K. Ramasesha, S. R. Leone, and D. M. Neumark, Annu. Rev. Phys. Chem. **67**, 41 (2016).